IOPscience iopscience.iop.org

Home Search Collections Journals About Contact us My IOPscience

Bottom Electrode Modification of ZrO_2 Resistive Switching Memory Device with Au Nanodots

This content has been downloaded from IOPscience. Please scroll down to see the full text.

2012 Jpn. J. Appl. Phys. 51 02BJ04

(http://iopscience.iop.org/1347-4065/51/2S/02BJ04)

View the table of contents for this issue, or go to the journal homepage for more

Download details:

IP Address: 140.113.38.11
This content was downloaded on 28/04/2014 at 21:49

Please note that terms and conditions apply.

DOI: 10.1143/JJAP.51.02BJ04

Bottom Electrode Modification of ZrO_2 Resistive Switching Memory Device with Au Nanodots

Dai-Ying Lee, I-Chuan Yao[1], and Tseung-Yuen Tseng*

Department of Electronics Engineering and Institute of Electronics, National Chiao Tung University, Hsinchu 300, Taiwan
[1] *Department of Materials Science and Engineering, National Chiao Tung University, Hsinchu 300, Taiwan*

Received September 14, 2011; accepted November 26, 2011; published online February 20, 2012

The resistive switching properties of the ZrO_2 memory devices with bottom electrode modification by using Au nanodots are investigated in this study. The regular arrays of Au nanodots are fabricated on Pt bottom electrode by nanosphere lithography. Due to the tip of the Au nanodots on the Pt bottom electrode, it causes the higher electric field within the ZrO_2 film above the nanodots due to reduced effective film thickness and induces the localized conducting filaments easily. The operation parameters' variation for switching devices is, therefore, suppressed with lower operation voltage and resistance ratio. Long retention time ($>10^6$ s) and stubborn nondestructive readout test ($>10^4$ s) at room temperature and 150 °C are also demonstrated in this device. © 2012 The Japan Society of Applied Physics

1. Introduction

Resistive random access memory (RRAM) device has been considered as a promising candidate to replace the present flash memory for next generation nonvolatile memory applications. RRAM utilizes two distinguishable resistive states (high conductive state, ON state and low conductive state, OFF state) to store digital data in unit cell. Furthermore, RRAM has advantages of long data retention, high-speed operation, thermal robustness, high scalability, and simple structure compatible with the standard complementary metal–oxide–semiconductor (CMOS) process.[1,2] However, there are large variations in switching parameters such as the resistance values of ON state (R_{on}) and OFF state (R_{off}), and the required voltages to switch from OFF state to ON state (V_{on}), and *vice versa* (V_{off}) needed to be solved for possibly practical application. So far, the detailed resistive switching (RS) mechanisms are arguable and unclear, where material properties and fabrication processes have significantly influence on them. The formation and rupture of conducting filaments with oxygen ions/vacancies migration within RRAM device are the most possible mechanism.[3–12] Therefore, based on this mechanism, several techniques were proposed to improve the operation parameters' variation, including modifying interface by active top electrode,[6] lowering effective film thickness by embedded metal technology,[7] reducing active device area by plug-bottom electrode,[8] stabilize local oxygen migrations by inserting IrO_2 buffer layer,[9] creating locally strong electric field by process control,[10] reducing the effective film thickness by Ni migration,[11] and changing structure by lightning rod effect.[12]

In this paper, we used nanosphere (NS) lithography to modify Pt bottom electrode with Au nanodots (Au:Pt) and fabricated the Pt/ZrO_2/Au:Pt device. NS lithography has merits of low cost and convenience in large-scale self-assembled nano-structure application.[13] The conducting filaments in the Pt/ZrO_2/Au:Pt device are believed to be easily induced above the Au nanodots on the Pt bottom electrode, where the electric field across the ZrO_2 film is the strongest. Hence, the conducting filaments are confined here, leading to less RS operation parameters' variation.

*E-mail address: tseng@cc.nctu.edu.tw

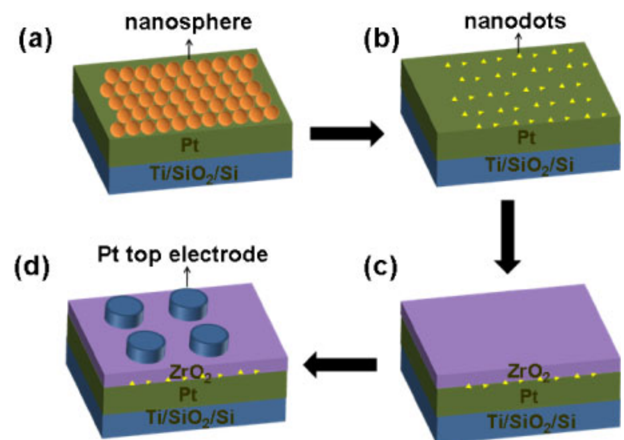

Fig. 1. (Color online) Schematic description of Pt/ZrO_2/Au:Pt device's fabrication procedures. (a) Before depositing Au metal, polystyrene NSs patterning to form the mask. (b) After depositing Au metal and then, removing NSs mask, the Au nanodots formed on the Pt bottom electrode. (c) Stacking ZrO_2 film on the modified bottom electrode. (d) Completed Pt/ZrO_2/Au:Pt device.

2. Experimental Procedure

Figure 1 depicts the processes of the Pt/ZrO_2/Au:Pt device fabrication. First, the polystyrene NSs order pattern was arranged on the Pt/Ti/SiO_2/Si substrate immersed with dispersed solution to form the mask. The scanning electron microscope (SEM; Hitachi S4700) image (inset of Fig. 2) shows neat arrangement of NSs on the Pt/Ti/SiO_2/Si substrate. After slowly lifting up the substrate from the solution, depositing Au metal by electron beam evaporation and then, removing NSs mask by dissolution in toluene, the Au nanodots formed on the Pt bottom electrode. The Au nanodots prepared by the NS lithography process were observed by SEM image as shown in Fig. 2. Sequentially, a 30-nm-thick ZrO_2 film was fabricated on this modified bottom electrode at 200 °C by a radio frequency magnetron sputtering. The base pressure of the sputtering chamber was below 2×10^{-5} Torr, and the deposition pressure was maintained at 10 mTorr with a gas mixture of oxygen and argon at a mixing ratio of 1 : 2 with a total flow of 18 sccm. A 30-nm-thick ZrO_2 film without Au nanodots was also fabricated as a reference sample. Finally, an 50-nm-thick Pt

 © 2012 The Japan Society of Applied Physics

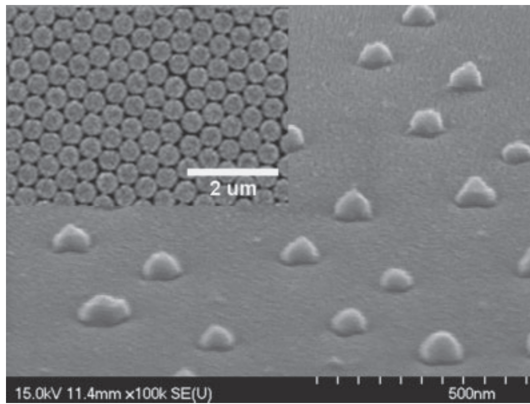

Fig. 2. SEM image of Au nanodots prepared by the NS lithography process. The inset shows neat arrangement of NSs on the $Pt/Ti/SiO_2/Si$ substrate.

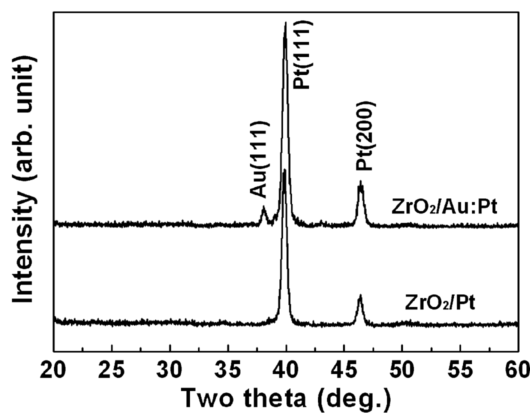

Fig. 3. XRD patterns of $Pt/ZrO_2/Pt$ and $Pt/ZrO_2/Au$:Pt devices.

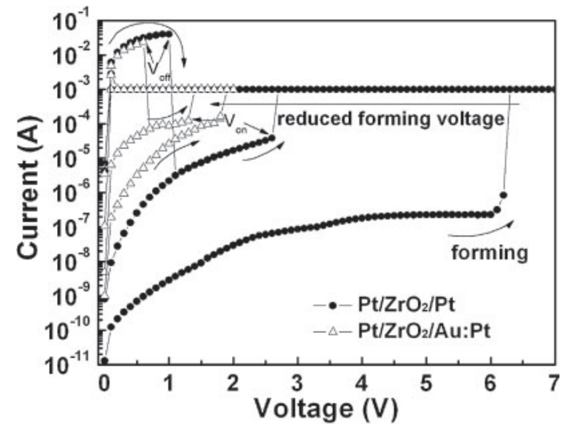

Fig. 4. Typical RS I–V curves of $Pt/ZrO_2/Pt$ and $Pt/ZrO_2/Au$:Pt devices.

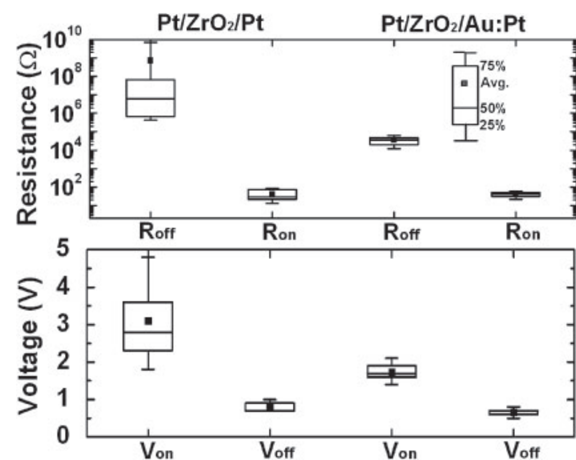

Fig. 5. Statistics of the RS operation parameters in $Pt/ZrO_2/Pt$ and $Pt/ZrO_2/Au$:Pt devices, respectively. R_{on} and R_{off} measured at 0.3 V for both devices.

top electrode was deposited by electron beam evaporation at ambient temperature with a diameter of 250 μm patterned by the shadow mask process to complete the $Pt/ZrO_2/Au$:Pt device. In order to confirm the crystalline phase and the orientation of the ZrO_2 films, X-ray diffraction (XRD; Rigaku RU-H3R) analyses were carried out. Agilent 4155C semiconductor parameter analyzer was used to measure the current–voltage (I–V) characteristics of the $Pt/ZrO_2/Au$:Pt memory device in ambient atmosphere at room temperature.

3. Results and Discussion

Figure 3 indicates the XRD patterns of the ZrO_2/Pt (reference sample) and the ZrO_2/Au:Pt, where both ZrO_2 films are amorphous. The peak of Au(111) is only observed in ZrO_2/Au:Pt, showing the existence of the Au nanodots. Although Au nanodots modify the morphology of the Pt bottom electrode, the micro-structure of the ZrO_2 film remains amorphous and unchanged. The forming process, similar to the soft breakdown, causes the conducting filaments created in the memory film with the highest electric field.[14–16] Hence, a high-voltage forming process with a current compliance of 1 mA is necessary. There is a sudden increase of current occurs near 6.2 V for the $Pt/ZrO_2/Pt$ device before performing any RS as shown in Fig. 4. Different from the $Pt/ZrO_2/Pt$ device, the forming voltage of the $Pt/ZrO_2/Au$:Pt device is reduced to about 1.9 V (close to V_{on}). The Au nanodots on Pt bottom electrode obviously lower the forming voltage. After finishing forming process, we apply a positive voltage to switch them to OFF state and back to ON state with a current compliance by applying another higher positive voltage. It is observed that the $Pt/ZrO_2/Au$:Pt device can be operated with lower voltages (V_{on} and V_{off}) than the $Pt/ZrO_2/Pt$ device.

Figure 5 demonstrates the statistical charts of the RS parameters during continuous RS by dc voltage in both $Pt/ZrO_2/Pt$ and $Pt/ZrO_2/Au$:Pt devices, respectively. Both R_{on} and R_{off} of the devices are measured at 0.3 V. The $Pt/ZrO_2/Au$:Pt device exhibits sharp distributions of R_{on}, R_{off}, V_{on}, and V_{off} and the corresponding dispersions are reduced compared with the $Pt/ZrO_2/Pt$ device. The stable RS indicates that the regions where the conducting filaments formed and ruptured are controlled and confined to some degree. For our $Pt/ZrO_2/Au$:Pt device, the strongest electric field across the ZrO_2 film is believed to exhibit near above the tip of the Au nanodots on the Pt bottom electrode, where the effective thickness of ZrO_2 film is reduced and the conducting filaments are easily induced after forming process. Then, the further occurrence of the conducting filaments formed and ruptured is confined here, causing less

© 2012 The Japan Society of Applied Physics

Table I. Summaries of the changes in R_{on}, R_{off}, V_{on}, V_{off}, and ratio (R_{off}/R_{on}) among the solutions to suppress the RS operation parameters' variation.

Solution	Device structure	R_{on}	R_{off}	V_{on}	$\lvert V_{off}\rvert$	Ratio	Ref.
Using Au nanodots	$Ti/ZrO_2/Au:Pt$	↑	↓	↓	↓	↓	This work
Using Ti top electrode	$Ti/ZrO_2/Pt$	↑	↓	↓	↓	↓	6
Embedding Cr layer	Al/SZO/Cr/SZO/LNO/Pt	↑	↓	↓	↓	↓	7
Using plug-BE	Pt/NiO/plug-BE	↑	↓	NA	NA	NA	8
Inserting IrO_2 buffer layers	$Pt/IrO_2/NiO/IrO_2/Pt$	↓	↓	↓	↓	↓	9
Process control	Pt/NiO/Pt	→	↓	↓	↓	↓	10
Alloy electrodes	$Ni_{0.83}Pt_{0.17}/NiO/Ni_{0.83}Pt_{0.17}$	↑	↓	↓	↓	↓	11
Using lightning rod effect	Cu/CuC/Pt	→	↓	↓	↓	↓	12

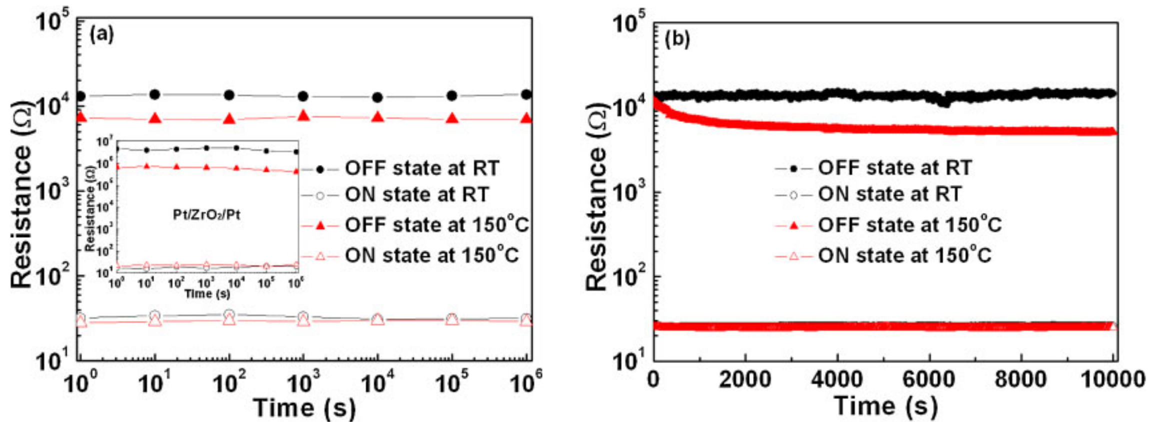

Fig. 6. (Color online) (a) Retention characteristics and (b) nondestructive readout properties of $Pt/ZrO_2/Au:Pt$ device measured at RT and 150 °C. Inset shows the retention characteristics of $Pt/ZrO_2/Pt$ device.

operation parameters' variation. Such an inner high electric field can also be created by embedding metal nanocrystals[17] and embedding Pt nanoparticles[18] within memory films, leading to stable RS behaviors.

Table I summarizes the current reported studies and their results of the changes in R_{on}, R_{off}, V_{on}, V_{off}, and resistance ratio (R_{off}/R_{on}). To suppress the RS operation parameters' variation by reducing and confining the effective RS region, several common phenomena are observed and concluded: (i) a decrease in operation voltage; (ii) a decrease in R_{off}; (iii) possibly a general increase in R_{on}; (iv) a total decrease in R_{off}/R_{on}. In spite of the decrease in R_{off}/R_{on}, it still provides an enough memory margin for RRAM application.

For retention characteristics, both ON state and OFF state of the $Pt/ZrO_2/Pt$ and the $Pt/ZrO_2/Au:Pt$ devices show no data loss for more than 10^6 s at room temperature (RT) and 150 °C, respectively as shown in Fig. 6(a). There is no significantly different in the retention characteristics between the $Pt/ZrO_2/Pt$ and the $Pt/ZrO_2/Au:Pt$ devices. In Fig. 6(b), both ON state and OFF state are almost kept at the same value under 0.3 V stress voltage at RT and 150 °C, respectively, and there are no observable degradation over 10^4 s. Hence, the $Pt/ZrO_2/Au:Pt$ device possesses robust ON state and OFF state for promising memory application.

4. Conclusions

In this study, the Pt bottom electrode modified with Au nanodots is proposed to suppress the variations in RS operation parameters, where the Au nanodots are prepared by NS lithography. The high electric field are created on above the tip of Au nanodots within $Pt/ZrO_2/Au:Pt$ device. The conducting filaments are believed to be possibly induced near above the tip of Au nanodots after forming process. Then, the conducting filaments are confined to decrease the operation parameters' variation. The retention characteristics and the nondestructive readout properties are also stable at both RT and 150 °C. The $Pt/ZrO_2/Au:Pt$ device shows a promising potential for next generation nonvolatile memory application.

Acknowledgment

This work was supported by the National Science Council, Taiwan, under project NSC 99-2221-E-009-166-MY3.

1) I. G. Baek, M. S. Lee, S. Seo, M. J. Lee, D. H. Seo, D. S. Suh, J. C. Park, H. S. Kim, I. K. Yoo, U. I. Chung, and J. T. Moon: IEDM Tech. Dig., 2004, p. 587.
2) H. Y. Lee, P. S. Chen, T. Y. Wu, Y. S. Chen, C. C. Wang, P. J. Tzeng, C. H. Lin, F. Chen, C. H. Lien, and M. J. Tsai: IEDM Tech. Dig., 2008, p. 297.
3) K. M. Kim, B. J. Choi, and C. S. Hwang: Appl. Phys. Lett. **90** (2007) 242906.
4) D. Y. Lee, S. Y. Wang, and T. Y. Tseng: J. Electrochem. Soc. **157** (2010) G166.
5) M. K. Yang, J. W. Park, T. K. Ko, and J. K. Lee: Appl. Phys. Lett. **95** (2009) 042105.
6) C. Y. Lin, C. Y. Wu, C. Y. Wu, T. C. Lee, F. L. Yang, C. Hu, and T. Y. Tseng: IEEE Electron Device Lett. **28** (2007) 366.
7) C. Y. Lin, M. H. Lin, M. C. Wu, C. H. Lin, and T. Y. Tseng: IEEE Electron Device Lett. **29** (2008) 1108.

 © 2012 The Japan Society of Applied Physics

8) I. G. Baek, D. C. Kim, M. J. Lee, H.-J. Kim, E. K. Yim, M. S. Lee, J. E. Lee, S. E. Ahn, S. Seo, J. H. Lee, J. C. Park, Y. K. Cha, S. O. Park, H. S. Kim, I. K. Yoo, U-In Chung, J. T. Moon, and B. I. Ryu: IEDM Tech. Dig., 2005, p. 769.
9) D. C. Kim, M. J. Lee, S. E. Ahn, S. Seo, J. C. Park, I. K. Yoo, J. G. Baek, H. J. Kim, E. Y. Yim, J. E. Lee, S. O. Park, H. S. Kim, U-In Chung, J. T. Moon, and B. I. Ryu: Appl. Phys. Lett. **88** (2006) 232106.
10) R. Jung, M. J. Lee, S. Seo, D. C. Kim, G. S. Park, K. Kim, S. Ahn, Y. Park, I. K. Yoo, J. S. Kim, and B. H. Parka: Appl. Phys. Lett. **91** (2007) 022112.
11) C. B. Lee, B. S. Kang, M. J. Lee, S. E. Ahn, G. Stefanovich, W. X. Xianyu, K. H. Kim, J. H. Hur, H. X. Yin, Y. Park, I. K. Yoo, J. B. Park, and B. H. Park: Appl. Phys. Lett. **91** (2007) 082104.
12) J. Park, M. Jo, J. Lee, S. Jung, S. Kim, W. Lee, J. Shin, and H. Hwang: IEEE Electron Device Lett. **32** (2011) 63.
13) W. Frey, C. K. Woods, and A. Chilkoti: Adv. Mater. (Weinheim, Ger.) **12** (2000) 1515.
14) C. Y. Lin, D. Y. Lee, S. Y. Wang, C. C. Lin, and T. Y. Tseng: Surf. Coatings Technol. **203** (2008) 628.
15) R. E. Thurstans and D. P. Oxley: J. Phys. D **35** (2002) 802.
16) K. Kinoshita, T. Tamura, M. Aoki, Y. Sugiyama, and H. Tanaka: Appl. Phys. Lett. **89** (2006) 103509.
17) Y. T. Tsai, T. C. Chang, C. C. Lin, S. C. Chen, C. W. Chen, S. M. Sze, F. S. Yeh, and T. Y. Tseng: Electrochem. Solid-State Lett. **14** (2011) H135.
18) M. Uenuma, K. Kawano, B. Zheng, N. Okamoto, M. Horita, S. Yoshii, I. Yamashita, and Y. Uraoka: Nanotechnology **22** (2011) 215201.

© 2012 The Japan Society of Applied Physics